

PREDICTION OF THREE-DIMENSIONAL FLOW AND HEAT TRANSFER THROUGH RIBBED DUCTS USING A NON-LINEAR $k-\epsilon$ MODEL

M. Raisee and H. Naeimi

Department of Mechanical Engineering, Faculty of Engineering,
University of Tehran, Tehran, Iran
mraisee@ut.ac.ir, hnaeimi@ut.ac.ir

H. Iacovides

School of Mechanical, Aerospace and Civil Engineering,
University of Manchester, Manchester, UK
h.iacovides@manchester.ac.uk

ABSTRACT

The present paper deals with the prediction of three-dimensional fluid flow and heat transfer in rib-roughened ducts of square cross-section. Such flows are of direct relevance to the internal cooling system of modern gas turbine blades. In this paper flow and thermal prediction of linear and non-linear $k-\epsilon$ models have been included. Both turbulence models have been used with the form of length-scale correction term to the dissipation rate originally proposed by Yap (1987) and also a differential version of this term, 'NYP'. The mean flow predictions show that both linear and non-linear $k-\epsilon$ models can successfully reproduce most of the measured data for stream-wise and cross-stream velocity components. Moreover, the non-linear model, which is sensitive to turbulence anisotropy, is able to produce better results for the turbulent stresses. Heat transfer comparisons show that the Nusselt number predictions obtained with the modified version of the non-linear eddy-viscosity model proposed by Craft et al. (1999) (NLEVM2) and the 'NYP' length-scale correction term are in close agreements with the measured data.

INTRODUCTION

Advanced gas turbine engines operate at high temperatures (2000 K) to improve thermal efficiency and power output. As the turbine inlet temperature increases, the heat transferred to the turbine blades also increases. Therefore, there is a need to cool the blades for safe operation. The blades are cooled by extracted air from the compressor of the engine. Three major cooling techniques are used for cooling turbine blades. The leading edge is cooled by jet impingement, the trailing edge is cooled by pin-fins, and the middle portion is cooled by rib-roughened coolant passages. The present study attempts to predict flow and heat transfer in internal rib-roughened passages of a gas turbine blade using a modified non-linear eddy-viscosity $k-\epsilon$ model.

Due to the practical relevance of flow and convective heat transfer in rib-roughened passages to the internal cooling of gas turbine blades, such flows have been the topic of extensive experimental and theoretical research. A number of experimental studies have concentrated on

detailed measurements of the local heat transfer coefficient, using liquid crystal techniques. A study which examined local heat transfer in ribbed ducts was conducted by Baughn and Yan (1992). Details of wall heat transfer on the ribbed and smooth walls in the developing and fully-developed regions were presented in the terms of two-dimensional plots and contours of local Nusselt number. In a similar study, Rau et al. (1998) employed a LDV system and a liquid crystal technique to provide flow field and local heat transfer data in the repeating flow region of a square-sectioned ducts roughened by normal ribs. The distribution of the local heat transfer on the ribbed and smooth walls showed features similar to those measured by Baughn and Yan (1992). Another experimental study which provided flow field and local heat transfer measurements in ribbed ducts was reported by Iacovides et al. (1998). For a square-sectioned ribbed U-bend, they performed flow and heat transfer measurements. Only the two ribbed walls were heated. In the straight upstream section of the ribbed duct, the Nusselt number was found to be high in the middle of each rib interval, where according to the LDA measurement the flow had reattached.

Most of the earlier numerical studies cited in the literature used two-dimensional solvers and employed high-Reynolds number turbulence models with wall-functions for their predictions. One example of such works is Liou et al. (1993). Two-dimensional numerical representations of flow and heat transfer through these ribbed passages are not entirely representative since these types of simulation ignore the three-dimensional effects on the flow and thermal behaviour. To arrive at numerical prediction methods reliable enough for thermal simulations in blade cooling passages, it is necessary to apply existing and emerging simulation strategies to three-dimensional flows through ribbed cooling passages. One of the first studies that examined three-dimensional flow and heat transfer in ribbed passages was performed by Iacovides (1998). Three-dimensional numerical predictions for turbulent flow and heat transfer through fully-developed stationary and rotating ribbed ducts with normal ribs in "in-line" and "staggered" arrangements were produced, using 2-layer $k-\epsilon$ and 2nd-moment (DSM) turbulence models. Both turbulence models produced satisfactory mean flow predictions. The predicted

Table 1: Details of the flow parameters of the 3D ribbed ducts examined.

Duct geometry	P/h	h/H	Re	Pr
in-line	10	0.0625	5.0×10^4	0.71
staggered	10	0.1	1.0×10^5	0.71

local heat transfer coefficients of both turbulence models were lower than the measured values, but the zonal DSM returned a more realistic profile for the local Nusselt number. In a subsequent study, Iacovides and Raisee (1999) showed that the most reliable flow and thermal predictions are produced through the use of low-Reynolds number 2nd-moment closures. More recently, large eddy simulation (LES) and also detached eddy simulation (DES) studies of cooling flows through ribbed passages have started to appear such as those of Sewall and Tafti (2004) and Ahn et al. (2005). The LES approach provides another, though computationally more demanding, alternative for the reliable computation of cooling flows in ribbed passages. A more detailed review of recent numerical studies can be found in Iacovides and Launder (2007).

Here a more economical way to capture turbulence anisotropy is explored, through the use of non-linear two-equation turbulence models. The stress-strain relation of the linear eddy-viscosity model is extended, by including non-linear products of strain and vorticity terms. These non-linear stress-strain relations produce differences in the normal stresses and thus extend the model's applicability to flows in which the anisotropy of turbulence is important. Craft et al. (1996) developed a non-linear eddy-viscosity model (NLEVM1), including low-Reynolds-number effects. Moreover, they demonstrated that, in order to exhibit the correct sensitivity to streamline curvature, cubic terms must be retained in the stress-strain relationship. The majority of alternative proposals only include quadratic terms. This model, in a range of applications including flow in curved channels, a rotating channel, transitional flow over a flat plate and impinging jet flow and flow around a turbine blades resulted in significant predictive improvements in comparison to the linear $k-\varepsilon$ model. However, parallel application of this model to computations of heat and fluid flow in ribbed passages by Raisee (1999) and an abrupt pipe expansion, by Cooper (1997), showed that it exhibited severe problems of numerical stability and also of predictive accuracy of the thermal behaviour.

In a subsequent study, Craft et al. (1999) considered the application of the non-linear model to separated and impinging flows. They modified the formulation for the variation of the turbulent viscosity parameter, c_μ , with the strain rate. The 'Yap', length-scale correction term, was replaced with a differential version of Iacovides and Raisee (1999). The modified model (NLEVM2) improved the thermal predictions in both an abrupt pipe expansion and also the axi-symmetric impinging jet, and also removed the numerical instability and the need to prescribe the wall-distance. Raisee et al. (2004) subsequently applied NLEVM2 to the prediction of heat and fluid flow in two-dimensional and axi-symmetric rib-roughened passages and found that marked improvements in thermal predictions can

be achieved in comparison to the original version of the non-linear EVM (NLEVM1).

The objective here is to further assess the non-linear model, (NLEVM2), in thermal predictions in three-dimensional rib-roughened ducts with normal ribs.

CASES EXAMINED

Here two different configurations are considered, namely: (I) a square duct with ribs normal to the flow direction in an "in-line" fashion (Figure 1(a)), and (II) a square duct with normal ribs in a "staggered" arrangement (Figure 1(b)). The symbol h denotes the rib height, w the rib width, P the rib spacing, W the channel width and H the channel height. A constant heat flux boundary condition is imposed for the top, bottom and side walls of the first duct as well as for the ribs' surfaces. For the second configuration constant heat flux was imposed on the ribbed walls, while the smooth walls and rib surfaces were thermally insulated. All relevant geometrical and flow parameters are listed in Table 1.

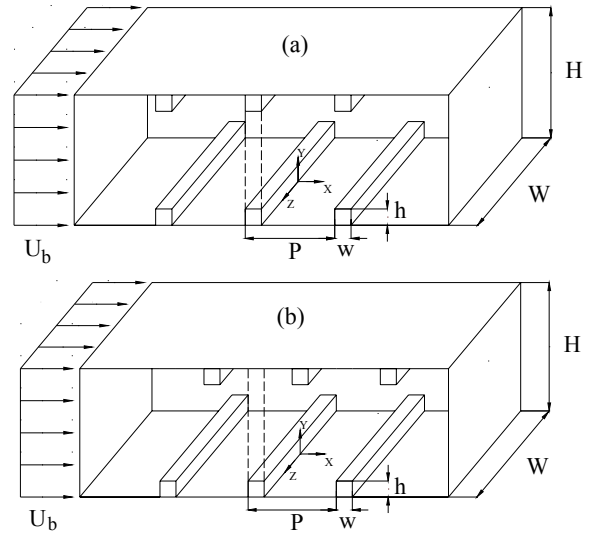


Figure 1: Three-dimensional ribbed ducts with normal ribs.

TURBULENCE MODELS

For a steady incompressible flow the conservation laws of mass, momentum and energy may be written as:

$$\frac{\partial U_j}{\partial x_j} = 0 \quad (1)$$

$$\frac{\partial (U_j U_i)}{\partial x_j} = \frac{-1}{\rho} \frac{\partial P}{\partial x_i} + \frac{\partial}{\partial x_j} \left(\nu \frac{\partial U_i}{\partial x_j} - u_i u_j \right) \quad (2)$$

$$\frac{\partial (U_j \Theta)}{\partial x_j} = \frac{\partial}{\partial x_j} \left(\frac{\nu}{Pr} \frac{\partial \Theta}{\partial x_j} - u_j \theta \right) \quad (3)$$

where ρ , ν and Pr are respectively, the density, the kinematic viscosity, and the Prandtl number of the fluid.

The turbulence model employed is the Craft et al. (1999) non-linear low-Reynolds-number $k-\varepsilon$ model (NLEVM2). The linear $k-\varepsilon$ model (EVM) of Launder and Sharma (1974) is also used as a reference. Furthermore, variants of the Yap term are tested.

Table 2: Empirical constants for the $k - \varepsilon$ model.

c_μ	$c_{\varepsilon 1}$	$c_{\varepsilon 2}$	σ_k	σ_ε	σ_θ
0.09	1.44	1.92	1	1.3	0.9

Table 3: Coefficients in the non-linear $k - \varepsilon$ model.

c_1	c_2	c_3	c_4	c_5	c_6	c_7
-0.1	0.1	0.26	$-10c_\mu^2$	0	$-5c_\mu^2$	$5c_\mu^2$

Linear low-Reynolds-number $k - \varepsilon$ model (EVM)

The Reynolds stresses and turbulent heat fluxes are obtained from:

$$\overline{-u_i u_j} = \nu_t \left(\frac{\partial U_i}{\partial x_j} + \frac{\partial U_j}{\partial x_i} \right) - \frac{2}{3} \delta_{ij} k \quad (4)$$

$$\overline{-u_i \theta} = \frac{\nu_t}{\sigma_\theta} \frac{\partial \theta}{\partial x_i} \quad (5)$$

where the turbulent viscosity, ν_t , is obtained from:

$$\nu_t = c_\mu f_\mu \frac{k^2}{\varepsilon} \quad (6)$$

and the values of constants c_μ and σ_θ are given in Table 2.

The transport equations for turbulent kinetic energy and dissipation rate ε , needed for ν_t , are:

$$\frac{\partial}{\partial x_j} (U_j k) = \frac{\partial}{\partial x_j} \left[\left(\nu + \frac{\nu_t}{\sigma_k} \right) \frac{\partial k}{\partial x_j} \right] + P_k - \varepsilon - 2\nu \left(\frac{\partial \sqrt{k}}{\partial x_j} \right)^2 \quad (7)$$

$$\begin{aligned} \frac{\partial}{\partial x_j} (U_j \varepsilon) &= \frac{\partial}{\partial x_j} \left[\left(\nu + \frac{\nu_t}{\sigma_\varepsilon} \right) \frac{\partial \varepsilon}{\partial x_j} \right] \\ &+ c_{\varepsilon 1} f_1 \frac{\varepsilon}{k} P_k - c_{\varepsilon 2} f_2 \frac{\varepsilon^2}{k} + E + S_\varepsilon \end{aligned} \quad (8)$$

P_k is the generation rate of k obtained from:

$$P_k = \overline{-u_i u_j} \frac{\partial U_i}{\partial x_j} \quad (9)$$

The damping functions f_μ , f_1 and f_2 are given by:

$$\begin{aligned} f_\mu &= \exp[-3.4/(1 + 0.02\tilde{R}_t)^2] \\ f_1 &= 1, \quad f_2 = 1 - 0.3 \exp(-\tilde{R}_t^2) \end{aligned} \quad (10)$$

where $\tilde{R}_t = k^2 / \nu \varepsilon$ is the local turbulent Reynolds number and the model constants are given in Table 2.

The term E , Jones and Launder (1972), is expressed as:

$$E = 2\nu \nu_t \left(\frac{\partial^2 U_i}{\partial x_j \partial x_k} \right)^2 \quad (11)$$

The extra source term, S_ε , stands for the ‘Yap’ correction term which is discussed in the later sections.

Modified non-linear low-Re $k - \varepsilon$ model (NLEVM2)

The turbulent stresses are obtained from:

$$\begin{aligned} \overline{-u_i u_j} &= \frac{2}{3} k \delta_{ij} - \nu_t S_{ij} + c_1 \frac{\nu_t k}{\varepsilon} \left(S_{ik} S_{kj} - \frac{1}{3} S_{kl} S_{kl} \delta_{ij} \right) \\ &+ c_2 \frac{\nu_t k}{\varepsilon} \left(\Omega_{ik} S_{kj} + \Omega_{jk} S_{ki} \right) + c_3 \frac{\nu_t k}{\varepsilon} \left(\Omega_{ik} \Omega_{jk} - \frac{1}{3} \Omega_{lk} \Omega_{lk} \delta_{ij} \right) \\ &+ c_4 \frac{\nu_t k^2}{\varepsilon^2} \left(S_{ki} \Omega_{lj} + S_{kj} \Omega_{li} \right) S_{kl} \\ &+ c_5 \frac{\nu_t k^2}{\varepsilon^2} \left(\Omega_{il} \Omega_{lm} S_{mj} + S_{il} \Omega_{lm} \Omega_{mj} - \frac{2}{3} S_{lm} \Omega_{mn} \Omega_{nl} \delta_{ij} \right) \\ &+ c_6 \frac{\nu_t k^2}{\varepsilon^2} S_{ij} S_{kl} S_{kl} + c_7 \frac{\nu_t k^2}{\varepsilon^2} S_{ij} \Omega_{kl} \Omega_{kl} \end{aligned} \quad (12)$$

where S_{ij} and Ω_{ij} are strain and vorticity rate tensors and model coefficients, $c_1 - c_7$, are given in Table 3.

The turbulent heat fluxes, $\overline{-u_i \theta}$, are modelled using the simple eddy-diffusivity approximation (equation 5).

The k and ε transport equations and eddy-viscosity formulation are similar to those of the EVM; however, the following modifications are proposed.

Modelling of c_μ . In a departure from the original NLEVM1, the following c_μ function was proposed by Craft et al. (1999):

$$c_\mu = \min[0.09, 1.2/(1 + 3.5\eta + f_{RS})] \quad (13)$$

where

$$\eta = \max\left(\frac{k}{\varepsilon} \sqrt{0.5 S_{ij} S_{ij}}, \frac{k}{\varepsilon} \sqrt{0.5 \Omega_{ij} \Omega_{ij}}\right) \quad (14)$$

$$f_{RS} = 0.235[\max(0, \eta - 3.333)]^2 \exp(-\tilde{R}_t / 400) \quad (15)$$

Near-wall damping. In the non-linear two equation model, the viscous damping function f_μ is provided:

$$f_\mu = 1 - \exp[-(\tilde{R}_t / 90)^{1/2} - (\tilde{R}_t / 400)^2] \quad (16)$$

The near wall source term E is expressed as:

$$E = \begin{cases} 0.0022 \frac{\tilde{S} \nu_t k^2}{\varepsilon} \left(\frac{\partial^2 U_i}{\partial x_k \partial x_l} \right)^2 & \text{for } \tilde{R}_t \leq 250 \\ 0 & \text{for } \tilde{R}_t > 250 \end{cases} \quad (17)$$

Length-scale correction term. To overcome the tendency of low-Re models to predict excessively high levels of near-wall turbulence, Yap (1987) introduced an extra source term into the dissipation rate equation, based on the wall distance Y :

$$S_\varepsilon = [Yap] = 0.83 \frac{\varepsilon^2}{k} \max\left[\left(\ell/\ell_\varepsilon - 1\right)\left(\ell/\ell_\varepsilon\right)^2, 0\right] \quad (18)$$

where ℓ is the turbulent length-scale, $k^{3/2}/\varepsilon$ and $\ell_\varepsilon = 2.55Y$ is the equilibrium length-scale.

To eliminate the wall distance, a differential form was proposed by Iacovides and Raisee (1999):

$$S_\varepsilon = [NYP] = \max \left[C_\omega F(F+1)^2 \tilde{\varepsilon}^2 / k, 0 \right] \quad (19)$$

where

$$F = \{ [(\partial \ell / \partial x_i)(\partial \ell / \partial x_i)]^{1/2} - (d\ell_\varepsilon / dY) \} / c_\ell \quad (20)$$

represents the difference between the predicted length-scale gradient, and the “equilibrium length-scale gradient”, $d\ell_\varepsilon / dY$, defined by:

$$d\ell_\varepsilon / dY = c_\ell [1 - \exp(-B_\varepsilon R_t)] + B_\varepsilon c_\ell R_t \exp(-B_\varepsilon R_t) \quad (21)$$

where $c_\ell = 2.55$, $B_\varepsilon = 0.1069$ and the coefficient C_ω for the linear model retains the original value of 0.83 while for the non-linear k- ε is defined as:

$$C_\omega = \frac{0.83 \min(1, \tilde{R}_t / 5)}{[0.8 + 0.7(\eta' / 3.33)^4 \exp(-\tilde{R}_t / 12.5)]} \quad (22)$$

with $\eta' = \max(\tilde{S}, \tilde{\Omega})$ and:

$$\begin{aligned} \tilde{S} &= \max[k / \tilde{\varepsilon}, \sqrt{v} / \varepsilon] \sqrt{0.5 S_{ij} S_{ij}} \\ \tilde{\Omega} &= \max[k / \tilde{\varepsilon}, \sqrt{v} / \varepsilon] \sqrt{0.5 \Omega_{ij} \Omega_{ij}} \end{aligned} \quad (23)$$

NUMERICAL METHOD ASPECTS AND BOUNDARY CONDITIONS

The calculations presented in this paper were obtained using version of the STREAM-3D code of Lien & Leschziner (1994). It employs Finite-Volume (FV) methodology in a fully-collocated grid system. A bounded version of the QUICK scheme, developed by Iacovides (1997), is used for the approximation of convective terms. The pressure field is linked to that of velocity through the well-known SIMPLE, algorithm. To avoid stability problems associated with pressure-velocity decoupling, the Rhie and Chow (1983) interpolation scheme is also employed. The flows considered in the present study are assumed to be periodic. Thus, computations are carried out in only one rib interval. The periodicity of the flow is imposed by equating the values of each variable (except temperature and pressure) at nodes just upstream and downstream of the inlet plane to the nodal values upstream and downstream of the output plane.

RESULTS AND DISCUSSION

The computed velocity field using the NLEVM2 in the mid-span ($Z/W = 0.0$) of the ducts with “staggered” ribs is displayed in Figure 2. For this configuration the sudden expansion after each rib creates a fairly large recirculation bubble downstream of the rib. The separated flow reattaches onto the wall at around $X/P = 0.4$. The flow also separates as it approaches the next rib, creating a smaller recirculation bubble in front of the rib.

In Figure 3, the predicted stream-wise and cross-stream velocity profiles for the duct with “staggered” ribs, using the EVM and NLEVM2, are compared with the measured data of Iacovides et al. (1998). The mean flow predictions of both models are similar and, in good agreement with the experimental data, except over the rib, where the cross-stream velocities are under-predicted by both models.

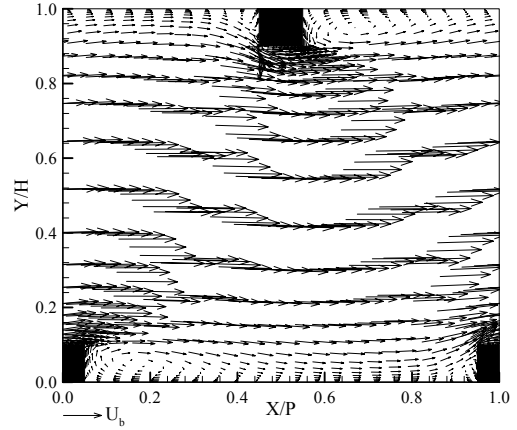


Figure 2: Velocity vectors along the mid-span of the duct with “staggered” ribs using NLEVM2 with ‘NYP’.

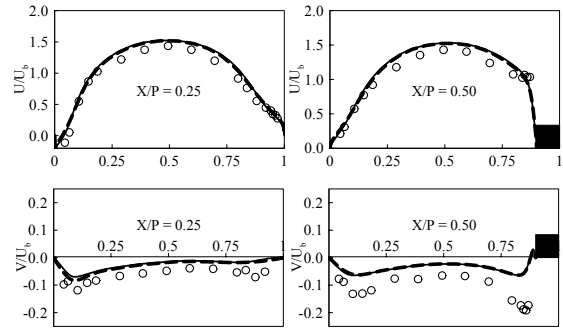


Figure 3: Velocity profiles for air flow through the duct with “staggered” ribs, --- EVM with ‘NYP’, — NLEVM2 with ‘NYP’, o Expt. Iacovides et al. (1998).

Figure 4 shows the predicted turbulence intensity and turbulent shear stress profiles in the symmetry plane of the duct with “staggered” ribs. Both models predict the very high, in comparisons to those in a duct with smooth walls, levels of turbulence intensities and turbulent shear stress, present in the measurements. The linear EVM, as expected, returns identical distributions for the stream-wise and cross-stream intensities $\sqrt{u^2} / U_b$ and $\sqrt{v^2} / U_b$ respectively. The non-linear model, NLEVM2, in closer accord with the data, produces an anisotropic turbulence field. The computed values of the cross-stream component of the turbulence intensity, $\sqrt{v^2} / U_b$, with both EVM and NLEVM2 models are similar and close to the measured data. Within the separation bubble, at $X/P = 0.25$, the cross-stream turbulence intensity is somewhat under-predicted by the NLEVM2.

For the stream-wise component, $\sqrt{u^2} / U_b$, the differences in the two sets of predictions are noticeable. The non-linear model, NLEVM2, in agreement with the measurements, returns higher stream-wise turbulence intensity levels near the two ribbed walls. Comparisons for the turbulent shear stress, \overline{uv} / U_b^2 , levels show that except for the region over the rib, where shear stress levels are under-estimated, the profiles returned by both turbulence models are in good agreement with the experimental data.

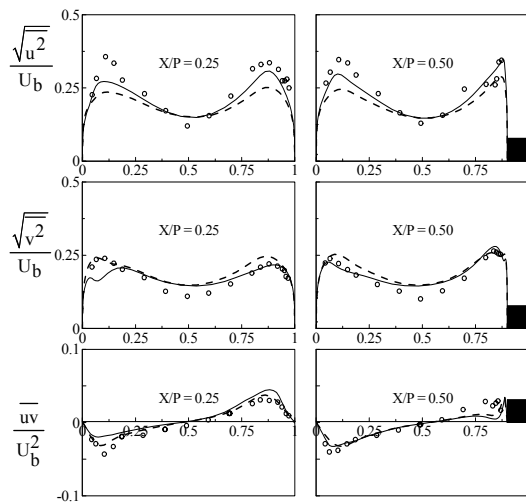


Figure 4: Turbulence intensity profiles for air flow through the duct with "staggered" ribs. Legend as in Figure 3.

The models tested produce similar and satisfactory predictions of the mean flow field, with some differences emerging in the predictions of the turbulence field. The non-linear model is in closer agreement with the measurements.

Figure 5 shows comparisons between the measured (Baughn and Yan (1992)) and the predicted Nusselt number contours on the ribbed walls of the square duct with "in-line" ribs. Comparisons show similar Nu distributions between the two sets of predictions and also with the experimental data. The highest heat transfer, as expected, occurs on the top of each rib. Between consecutive ribs, both the EVM and NLEVM2 models, consistent with the experiment, produce a low heat transfer zone immediately downstream of the rib, followed by a high heat transfer region between the ribs, presumably associated with the flow re-attachment. In the span-wise direction (from the symmetry-line of ribbed wall towards the smooth side wall) the predicted Nusselt numbers gradually drops towards the smooth side wall, and eventually reaches its lowest level at the corner between the ribbed and smooth walls. This is possibly due to the fact that as one approaches the corner, the flow becomes less active, i.e. the momentum of the flow and the turbulence levels decrease. In the experimental data, in contrast to both computations, downstream of the rib, the high heat transfer levels recorded at the reattachment point, extend from the symmetry line over most of the span of the ribbed wall, towards the corners. This suggests that both models tested underestimate the secondary motion and, consequently, the turbulence levels in the corner regions.

In Figure 6 the computed center-line Nusselt number variations, using EVM and NLEVM2 with both 'Yap' and 'NYP' are compared with the experimental data of Baughn and Yan (1992). The results of both models, and especially those of NLEVM2, are in better agreement with the measurements. Within the recirculation bubble, computations with both models and the 'NYP' term still overestimate the Nusselt numbers. On the other hand, outside the separation bubble (i.e. $X/P > 0.4$) while the EVM somewhat underestimates the heat-transfer levels, the NLEVM2 predictions are close to the measured values.

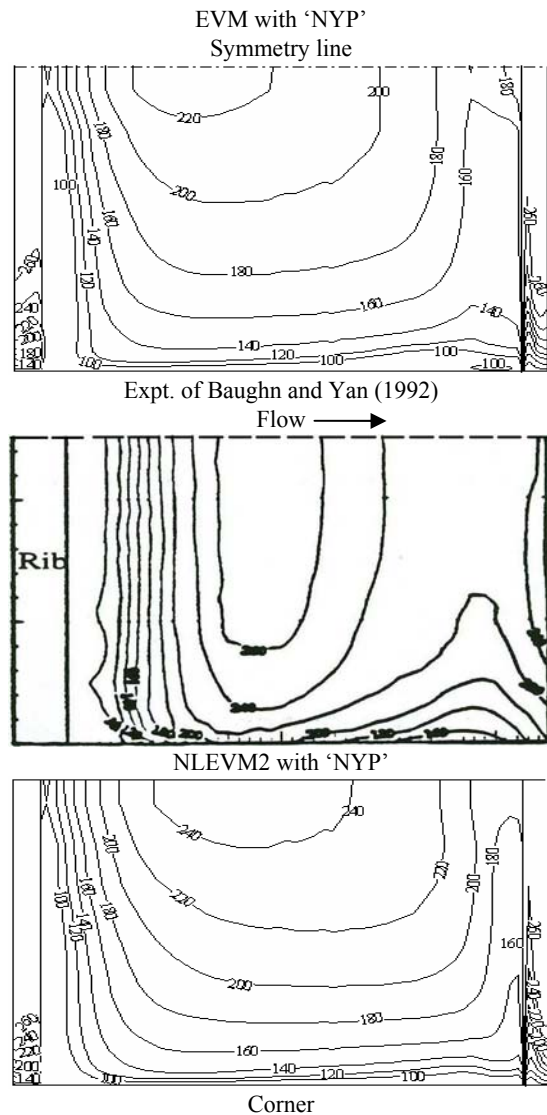


Figure 5: Comparison of computed and measured distributions of the local Nusselt number on the ribbed wall of the duct with "in-line" ribs.

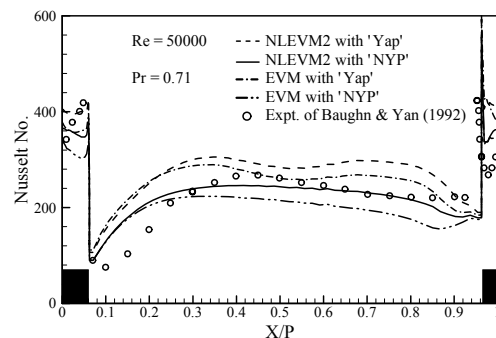


Figure 6: Predicted distribution of the centre-line Nusselt number through the duct with "in-line" ribs.

The same conclusion can be reached from Nusselt number comparisons presented in Figure 7 for air flow through the duct with "staggered" ribs. As found for the duct with "in-line" ribs, both models with the 'Yap' term

over-estimate the center-line Nusselt number. The center-line variation of the Nusselt number is best reproduced using the NLEVM2 model with the 'NYP' correction term.

The thermal predictions are consistent with those of the same models for flow through axi-symmetric and two dimensional ribbed passages; see Rasee et al. (2004). Both sets of comparisons thus suggest that the center-line Nusselt numbers are best reproduced using the NLEVM2 model with the 'NYP' correction term.

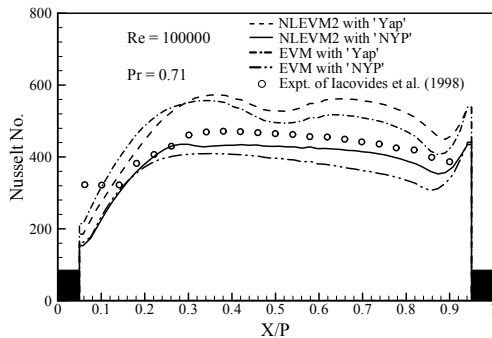


Figure 7: Predicted distribution of the centre-line Nusselt number through the duct with "staggered" ribs.

CONCLUSIONS

From the computational results presented it is found that both the EVM and NLEVM2 models were able to produce reliable velocity fields. As expected, the NLEVM2, which has some sensitivity to turbulence anisotropy, generally predicts the turbulence quantities more faithfully than the EVM. Of the two turbulence models considered, the heat transfer predictions of the recent version of cubic non-linear $k-\varepsilon$ model (NLEVM2) with the 'NYP' term are closer to the experimental data. Thus, this modified version of the non-linear $k-\varepsilon$ model that has been shown in earlier studies to improve the thermal predictions in two-dimensional and axi-symmetric ribbed passages, also produces reliable heat transfer predictions in three-dimensional ribbed ducts.

REFERENCES

Ahn, J., Choi, H., and Lee, J. S., 2005, "Large Eddy Simulation of Flow and Heat Transfer in a Channel Roughened by Square or Semi-Circular Ribs", *ASME J. of Turbomachinery*, Vol. 127, pp. 263-269.

Baughn, J. W., and Yan, X., 1992, "Local Heat Transfer Measurements in Square Ducts with Transverse Ribs", *Proceeding, 28th National Heat Transfer Conf. ASME, San Diego, California*, Vol. 202, pp. 1-7.

Cooper, D., 1997, "Computation of Momentum and Heat Transfer in a Separated Flow Using Low-Reynolds Number Linear and Non-Linear $k-\varepsilon$ Models", MRes Dissertation, Dept. of Mech. Engng., UMIST.

Craft, T. J., Launder, B. E., and Suga, K., 1996, "Development and Application of a Cubic Eddy Viscosity Model of Turbulence", *Int. J. of Heat and Fluid Flow*, Vol. 17, pp. 108-115.

Craft, T. J., Iacovides, H., and Yoon, J. H., 1999, "Progress in the Use of Non-Linear Two-Equation Models in the Computation of Convective Heat Transfer in

Impinging and Separated Flows", *Flow, Turbulence and Combustion*, Vol. 63, pp. 59-80.

Iacovides, H., 1997, "The Computation of Turbulent Flow through Stationary and Rotating U-bends of with Rib-Roughened Surfaces", *Proceeding, 11th Int. Conf. on Laminar and Turbulence Flows*, Swansea, U.K.

Iacovides, H., 1998, "Computation of Flow and Heat Transfer through Rotating and Stationary Passages", *Int. J. of Heat and Fluid Flow*, Vol. 19, pp. 393-400.

Iacovides, H., Jackson, D. C., Kelemenis, G., Launder, B. E., and Yuan, Y.-M., 1998, "Recent Progress in the Experimental Investigation of Flow and Local Wall Heat Transfer in Internal Cooling Passages of Gas-Turbine Blades", *Proceeding, 2nd Int. Conf. on Turbulent Heat Transfer*, Manchester, U.K., Vol. 2, 7.14 -7.28.

Iacovides, H., and Rasee, M., 1999, "Recent Progress in the Computation of Flow and Heat Transfer in Internal Cooling Passages of Turbine Blade", *Int. J. of Heat and Fluid Flow*, Vol. 20, pp. 320-328.

Iacovides H., and Launder B. E., 2007, "Internal Blade Cooling: the Cinderella of C&EFD Research in Gas Turbines", *Review Paper, Part A, J. of Power and Energy, To Appear*.

Jones, W. P., and Launder, B. E., 1972, "The Prediction of Laminarization with a Two Equation Model of Turbulence", *Int. J. Heat Mass Transfer*, Vol. 15, pp.301-14.

Launder, B. E., and Sharma, B. I., 1974, "Application of the Energy Dissipation Model of Turbulence to the Calculation of Flow Near a Spinning Disc", *Letters in Heat Mass Transfer*, Vol. 1, pp.131-138.

Lien, F. S., and Leschziner, M. A., 1994, "A General Non-Orthogonal Finite-Volume Algorithm for Turbulent Flow at All Speeds Incorporating Second-Moment Turbulence Transport Closure, Part 1: Numerical Implementation, and Part 2: Application", *Comp. Meth. in Applied Mech. Engng.*, Vol. 14, pp. 123-167.

Liou, T. M., Hwang, J. J., and Chen, S. H., 1993, "Simulation and Measurement of Enhanced Turbulent Heat Transfer in a Channel with Periodic Ribs on One Principal Wall", *Int. J. of Heat Mass Transfer*, Vol. 36, pp. 507-517.

Rasee, M., 1999, "Computation of Flow and Heat Transfer through Two & Three-dimensional Rib-Roughened Passages", Ph.D. Thesis, Dept. of Mech. Engng., UMIST.

Rasee, M., Noursadeghi, A., and Iacovides, H., 2004, "Application of Non-linear $k-\varepsilon$ Model in Prediction of Convective Heat Transfer through Ribbed Passages", *Int. J. Num. Meth. for Heat & Fluid Flow*, Vol. 14, pp. 285-304.

Rau, G., Cakan, M., Moeller, D., and Arts, T., 1998, "The Effects of Periodic Ribs on the Aerodynamic and Heat Transfer Performance on a Straight Cooling Channels", *ASME J. of Turbomachinery*, Vol. 120, pp. 368-375.

Rhie, C. M., and Chow, W. L., 1983, "Numerical Study of the Turbulent Flow Past an Airfoil with Trailing Edge Separation", *AIAA J.*, Vol. 21, pp. 1525-1532.

Sewall, E. A., and Tafti, D. K., 2004, "Large Eddy Simulation of the Developing Region of a Rotating Ribbed Internal Turbine Blade Cooling Channel", *Paper GT2004-53833, ASME Turbo Expo, Vienna, Austria*.

Yap, C. R., 1987, "Turbulent Heat and Momentum Transfer in Recirculating and Impinging Flows", Ph.D. Thesis, Faculty of Technology, University of Manchester.